

Mechanism of Plasmon-Driven Molecular Jackhammers in Mechanical Opening and Disassembly of Membranes— Supporting Information

Ciceron Ayala-Orozco,^{1,5*} Vardan Vardanyan,¹ Katherine Lopez-Jaime,² Zicheng Wang,¹ Jorge M. Seminario,^{2,3*} Anatoly B. Kolomeisky,^{1*} James M. Tour^{1,4*}

¹Department of Chemistry, Rice University; Houston, Texas 77005, USA

²Department of Chemical Engineering and Department of Electrical and Computer Engineering, Texas A&M University, College Station, Texas, 77843, USA

³Department of Materials Science and Engineering, Texas A&M University, College Station, Texas, 77843, USA

⁴Department of Materials Science and NanoEngineering, the NanoCarbon Center, the Smalley Curl Institute, and the Rice Advanced Materials Institute, Rice University; Houston, Texas 77005, USA

⁵The Molecular Jackhammer Cancer Therapeutics Institute, Houston, Texas 77230, USA

*Corresponding authors: ciceron.orozco@gmail.com; seminario@tamu.edu; tolya@rice.edu; tour@rice.edu

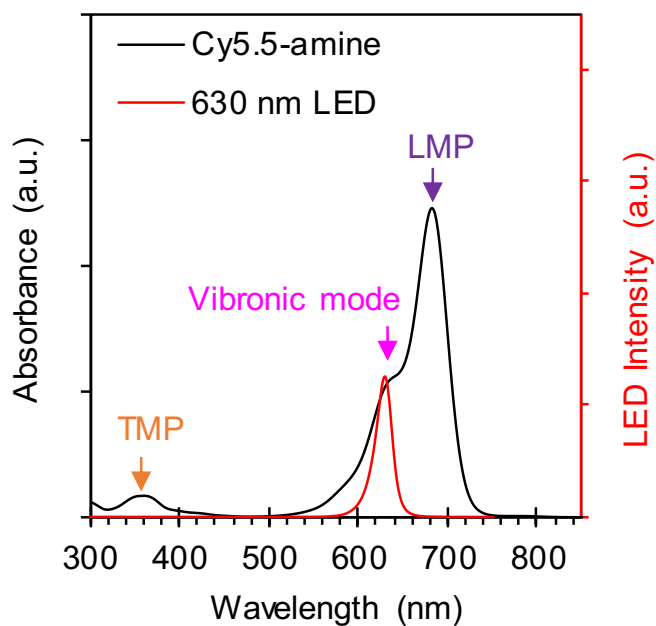


Figure S1. Absorption spectrum of Cy5.5-amine and emission spectrum of 630 nm LED. The positions of the transversal molecular plasmon (TMP) and longitudinal molecular plasmon (LMP) are assigned.

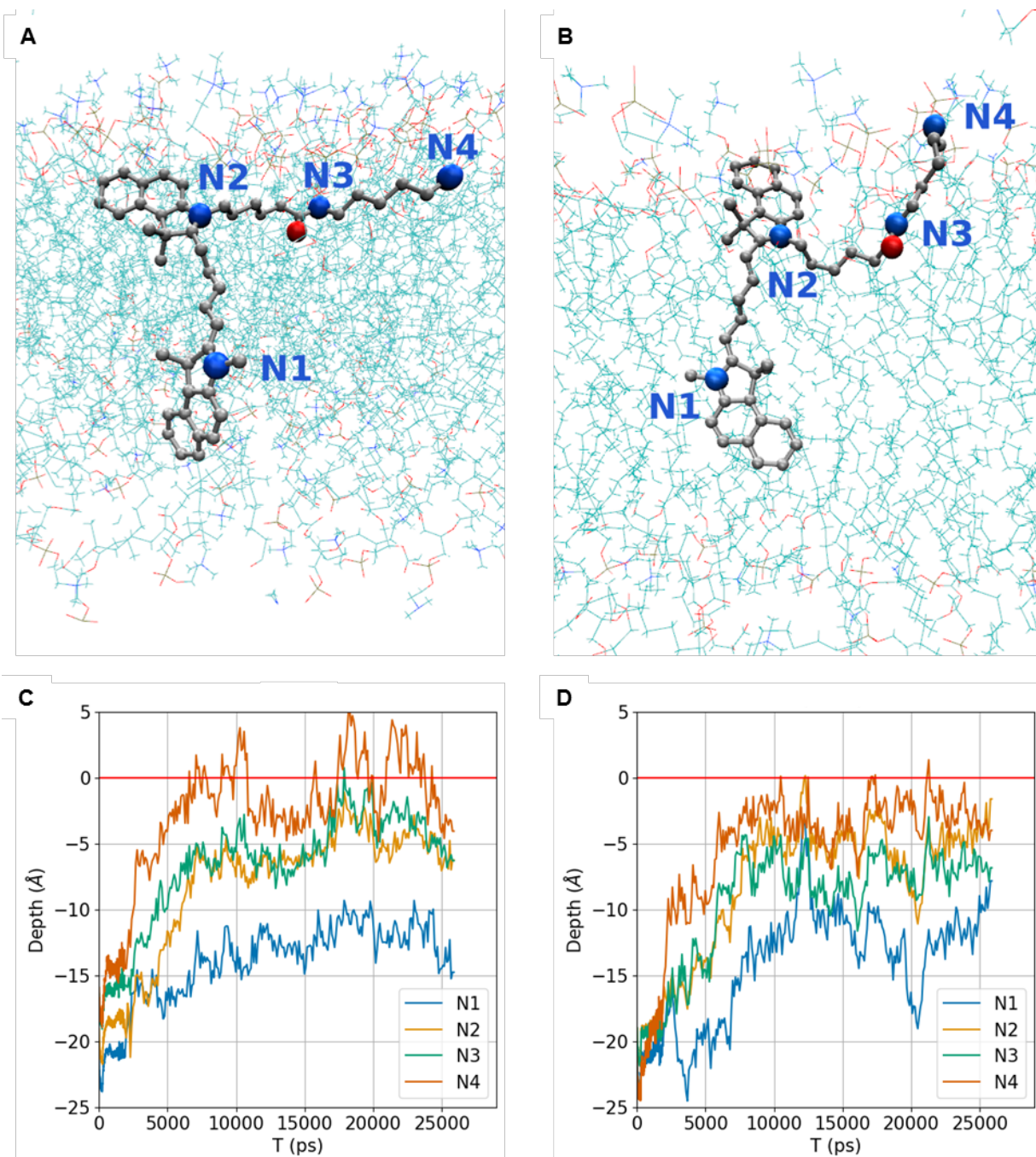


Figure S2. Molecular dynamics simulation of Cy5.5-amine inside a DPhPC membrane versus a POPC/POPE/POPG membrane. **A)** Representative position of Cy5.5-amine inside a DPhPC (1,2-diphytanoyl-*sn*-glycero-3-phosphocholine) membrane. Nitrogen is shown by blue atoms, carbon by grey atoms, and oxygen by a red atom. Nitrogen atoms are numerated. N2 and N4 are positively charged. **B)** Representative position of Cy5.5-amine inside a (1-palmitoyl-2-oleoyl-

glycero-3-phosphocholine/1-palmitoyl-2-oleoyl-*sn*-glycero-3-phosphoethanolamine/1-palmitoyl-2-oleoyl-*sn*-glycero-3-phospho-(1'-*rac*-glycerol)) (POPC/POPE/POPG) membrane. Nitrogen is shown by blue atoms, carbon by grey atoms, and oxygen by a red atom. Nitrogen atoms are numerated. N2 and N4 are positively charged. **C)** Evaluation of depths of the nitrogen atoms over the simulation time for Cy5.5-amine inside the DPhPC membrane. **D)** Evaluation of depths of the nitrogen atoms over the simulation time for Cy5.5-amine inside the POPC/POPE/POPG membrane. The zero level (red line) represents the membrane averaged over z coordinate of phosphate groups.

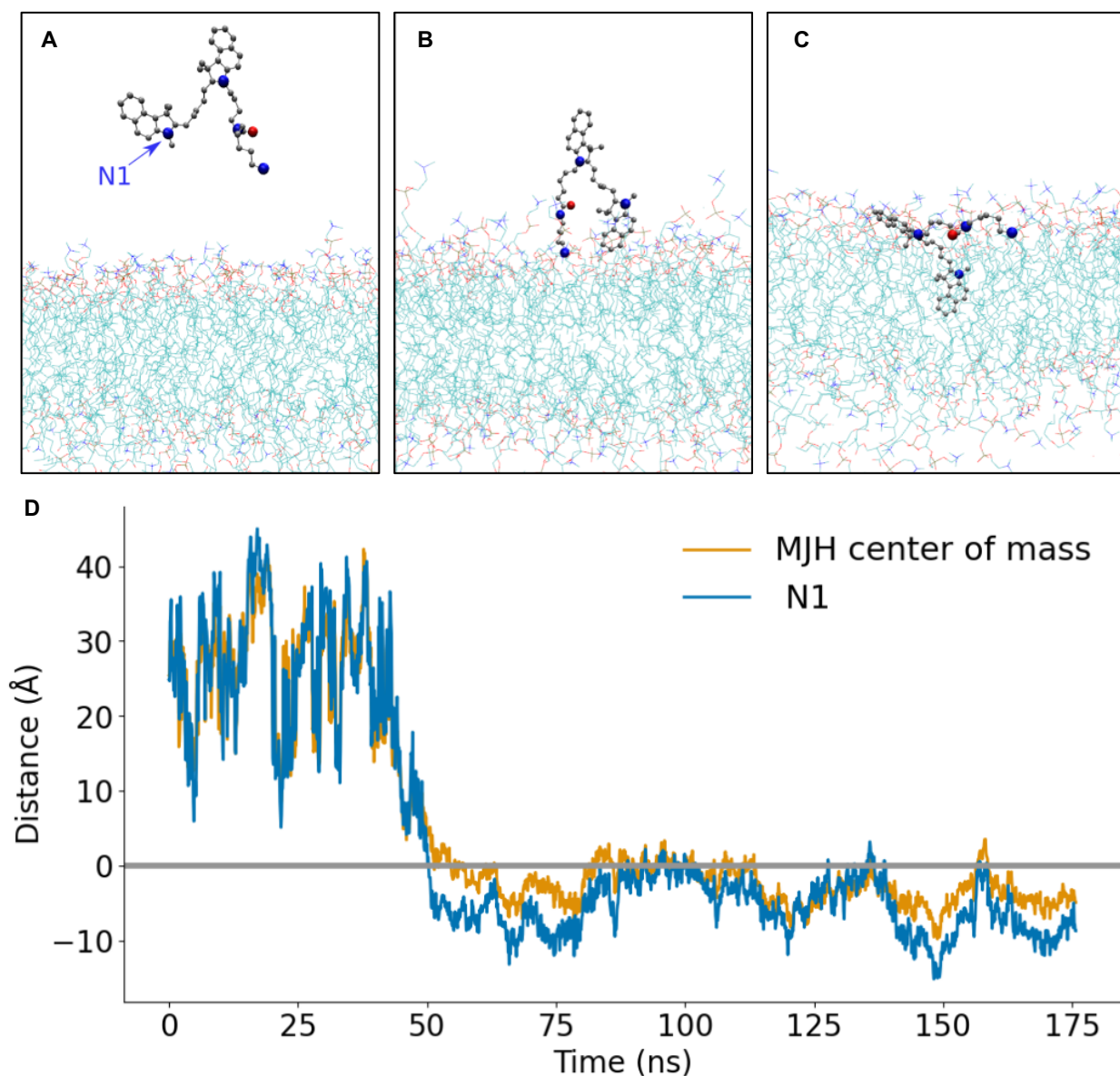


Figure S3. Molecular dynamics simulation of Cy5.5-amine starting outside a DPhPC membrane steps of insertion into the membrane. A) Representative position of Cy5.5-amine at the initial stage of the simulation relative to the DPhPC (1,2-diphytanoyl-*sn*-glycero-3-phosphocholine) membrane. Nitrogen is shown by blue atoms, carbon by grey atoms, and oxygen by a red atom. The position of the nitrogen atom labeled is analyzed over the simulation and the center of mass of the molecule. **B)** Representative position of Cy5.5-amine entering the DPhPC membrane. **C)** Representative position of Cy5.5-amine inside the DPhPC membrane. **D)** Analysis

of positions of the nitrogen atom N1 and the center of mass for Cy5.5-amine over the simulation time relative to the position of the DPhPC membrane. The zero level (grey line) represents the membrane's upper leaflet averaged over z coordinate of phosphate groups.

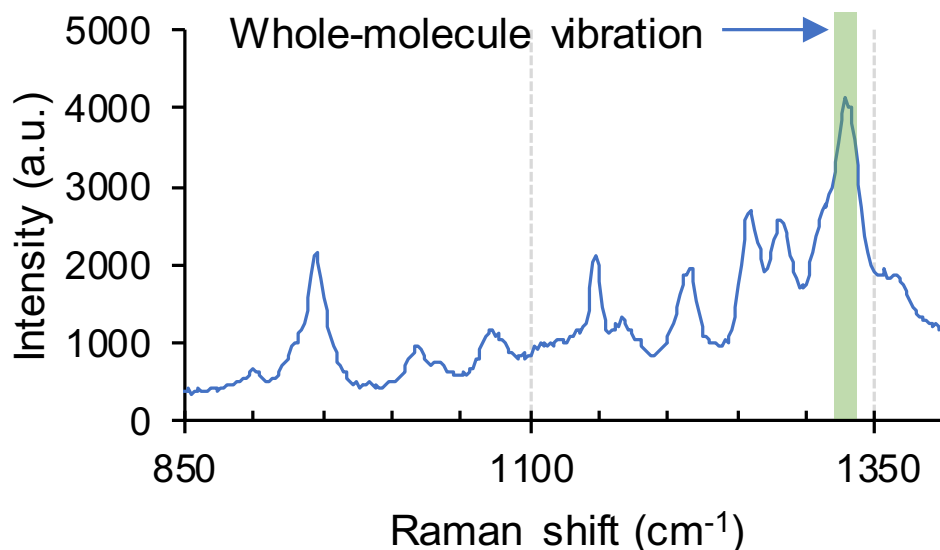


Figure S4. Raman spectrum of Cy5.5-amine. The whole-molecule concerted vibration of most cyanines is $\sim 1350 \text{ cm}^{-1}$ in the Raman spectrum.¹⁻³ This Raman spectrum was included in the Supporting Information in our previous study.³

Table S1. Oscillation frequency of the concerted-whole molecule vibration in Cy5.5-amine. The values are obtained from the Raman spectrum.³

Entry	Raman shift (cm^{-1})	Time of a single oscillation (fs)	Frequency (THz)	Energy (meV)
Cy5.5-amine	1330	25.08	40	164.9

The Raman shift values (cm^{-1}) obtained from the Raman spectrum were converted to the time required for a single oscillation (fs), the frequency (s^{-1}) and the energy (meV).

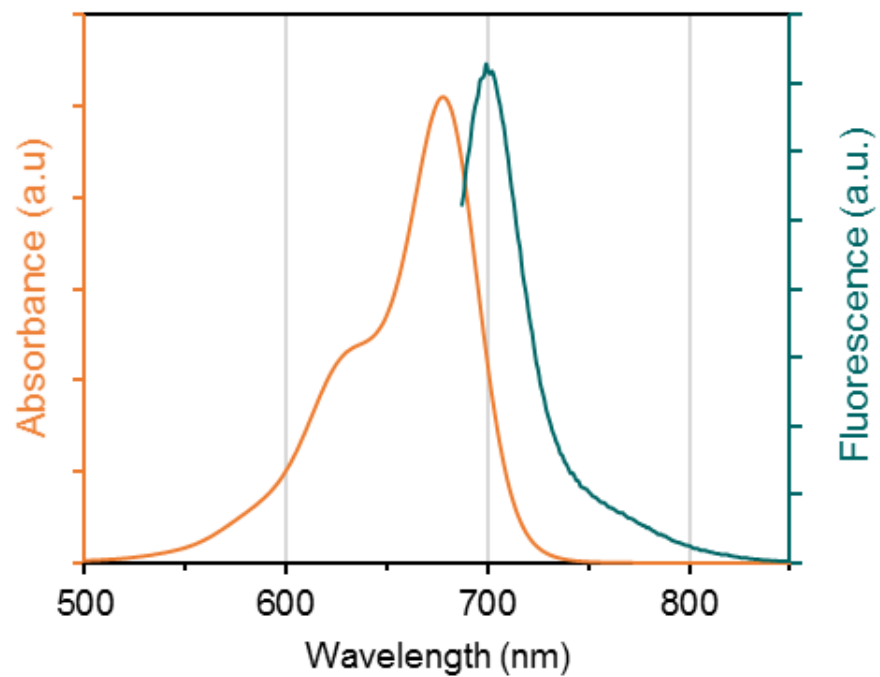


Figure S5. Absorption and fluorescence emission spectrum of Cy5.5-amine (2.7 μ M) in methanol. The peak of absorbance was $\lambda_{\text{abs}} = 678$ nm. For the fluorescence spectrum, $\lambda_{\text{ex}} = 667$ nm and $\lambda_{\text{em}} = 699$ nm.

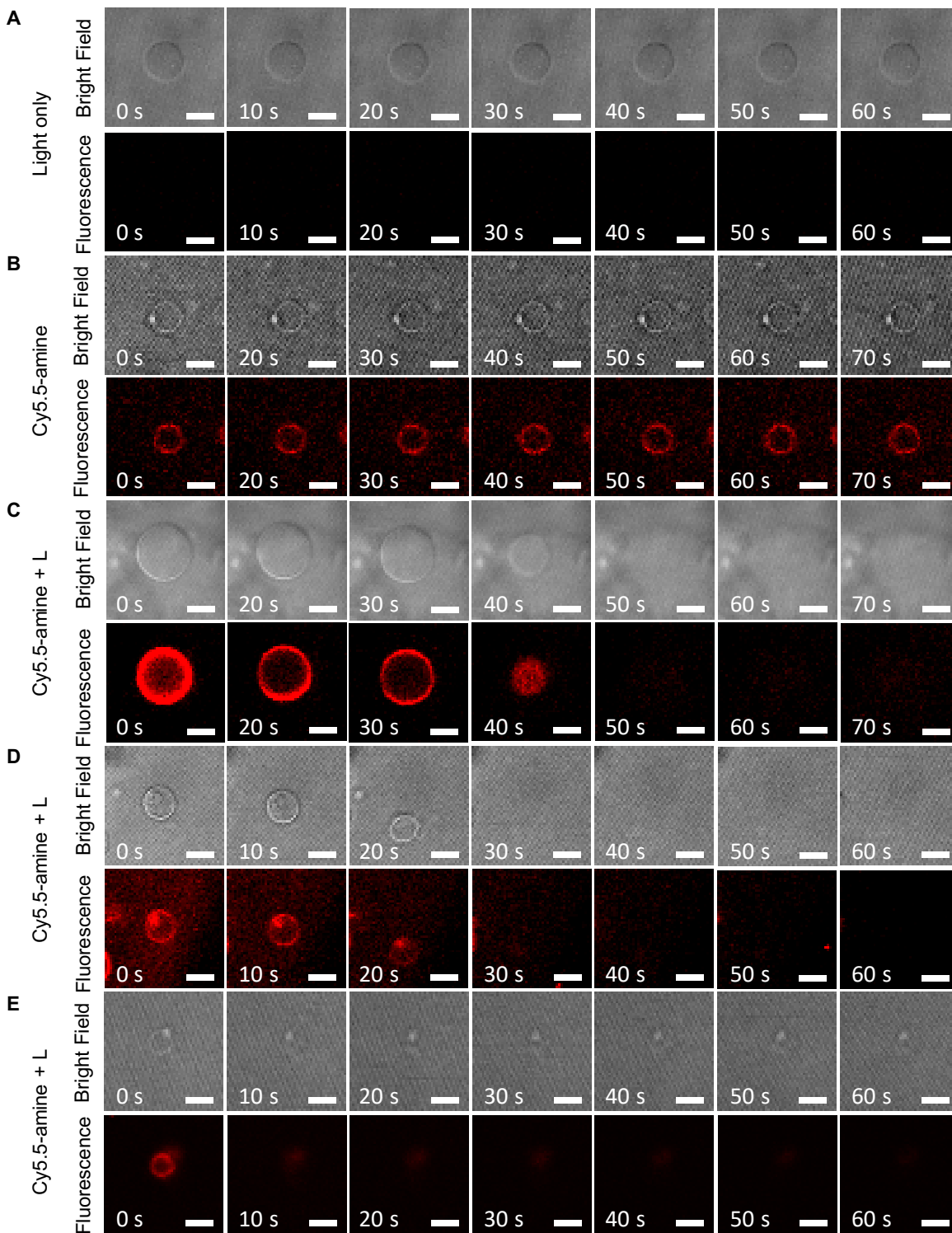


Figure S6. Time-course treatment of DPhPC GUUV with MJH Cy5.5-amine with and without light activation. The light activation consisted of laser scanning stimulation at 640 nm with a

confocal microscope laser at 5% power (50 μ W power, Plan Apo IR 60x/1.27 water immersion objective). The Cy5.5-amine localization was recorded by imaging at $\lambda_{\text{ex}} = 640$ nm, $\lambda_{\text{em}} = 663$ -738 nm, and 5% (50 μ W) laser power every 10 s. **A)** DPhPC GUV treated with 0.1% DMSO (no Cy5.5-amine) as control under light treatment. **B)** DPhPC GUV treated with 2 μ M Cy5.5-amine without light activation. **C)** DPhPC GUV of $r_0 = 4.9$ μ m treated with 2 μ M Cy5.5-amine under VDA photoactivation. **D)** DPhPC GUV of $r_0 = 2.8$ μ m treated with 2 μ M Cy5.5-amine under VDA photoactivation. **E)** DPhPC GUV of $r_0 = 1.9$ μ m treated with 2 μ M Cy5.5-amine under VDA photoactivation. The size of GUV is measured by the initial radius (r_0). The pictures were recorded every 10 s for all the panels. Scale bar 5 μ m. The tiny red dots in the fluorescence channel might be free Cy5.5-amine and/or background fluorescence. It is expected that the free Cy5.5-amine in the aqueous phase might have a lower fluorescent yield than the Cy5.5-amine inserted within the lipid membrane in a non-polar environment, a common behavior observed for free fluorophores *versus* those bound to biological structures.⁴

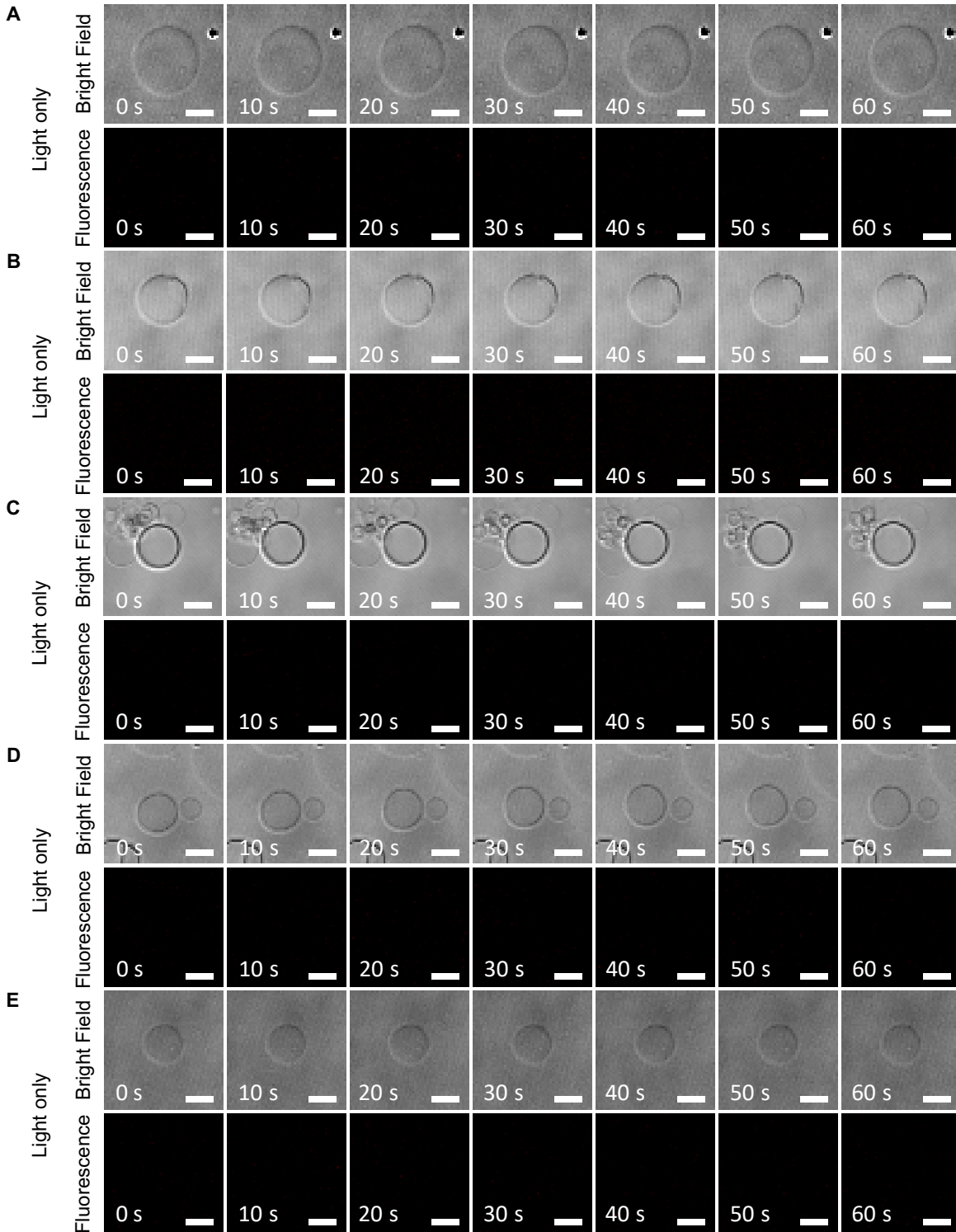


Figure S7. Time-course treatment of DPhPC GUV with light activation. The light activation consisted of laser scanning stimulation at 640 nm with a confocal microscope

laser at 5% power (50 μ W power, Plan Apo IR 60x/1.27 water immersion objective). DPhPC GUV treated with 0.1% DMSO in PBS buffer as control under light treatment for **A)** DPhPC GUV of $r_0 = 6.0 \mu\text{m}$, **B)** DPhPC GUV of $r_0 = 4.4 \mu\text{m}$, **C)** DPhPC GUV of $r_0 = 3.7 \mu\text{m}$, **D)** DPhPC GUV of $r_0 = 3.6 \mu\text{m}$, and **E)** DPhPC GUV of $r_0 = 3.2 \mu\text{m}$. The size of GUV is measured by the initial radius (r_0). The pictures were recorded every 10 s for all the panels. Scale bar 5 μm .

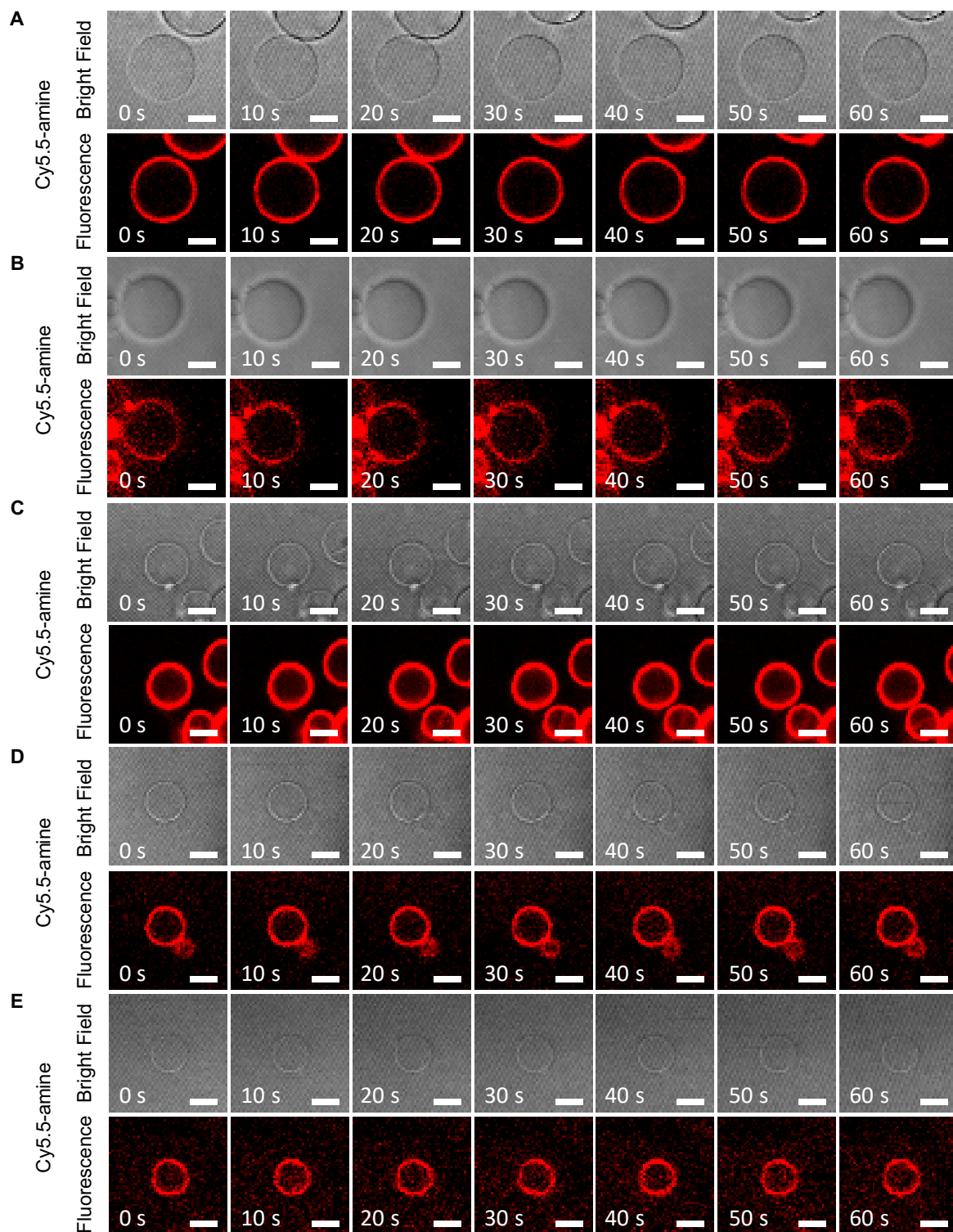


Figure S8. Time-course treatment of DPhPC GUV with MJH Cy5.5-amine without light activation. The Cy5.5-amine localization was recorded by imaging at $\lambda_{\text{ex}} = 640 \text{ nm}$,

$\lambda_{em} = 663-738$ nm, and 5% (50 μ W power, Plan Apo IR 60x/1.27 water immersion objective) laser power every 10 s (with a minor light exposure using a dwell time = 2.18 μ s). DPhPC GUV treated with 2 μ M Cy5.5-amine without light activation for **A)** DPhPC GUV of $r_0 = 5.8$ μ m, **B)** DPhPC GUV of $r_0 = 5.7$ μ m, **C)** DPhPC GUV of $r_0 = 3.7$ μ m, **D)** DPhPC GUV of $r_0 = 3.6$ μ m, and **E)** DPhPC GUV of $r_0 = 3.0$ μ m. The size of GUV is measured by the initial radius (r_0). The pictures were recorded every 10 s for all the panels. Scale bar 5 μ m. The tiny red dots in the fluorescence channel might be free Cy5.5-amine and/or background fluorescence. It is expected that the free Cy5.5-amine in the aqueous phase might have a lower fluorescent yield than the Cy5.5-amine inserted within the lipid membrane in a non-polar environment, a common behavior observed for free fluorophores *versus* those bound to biological structures.⁴

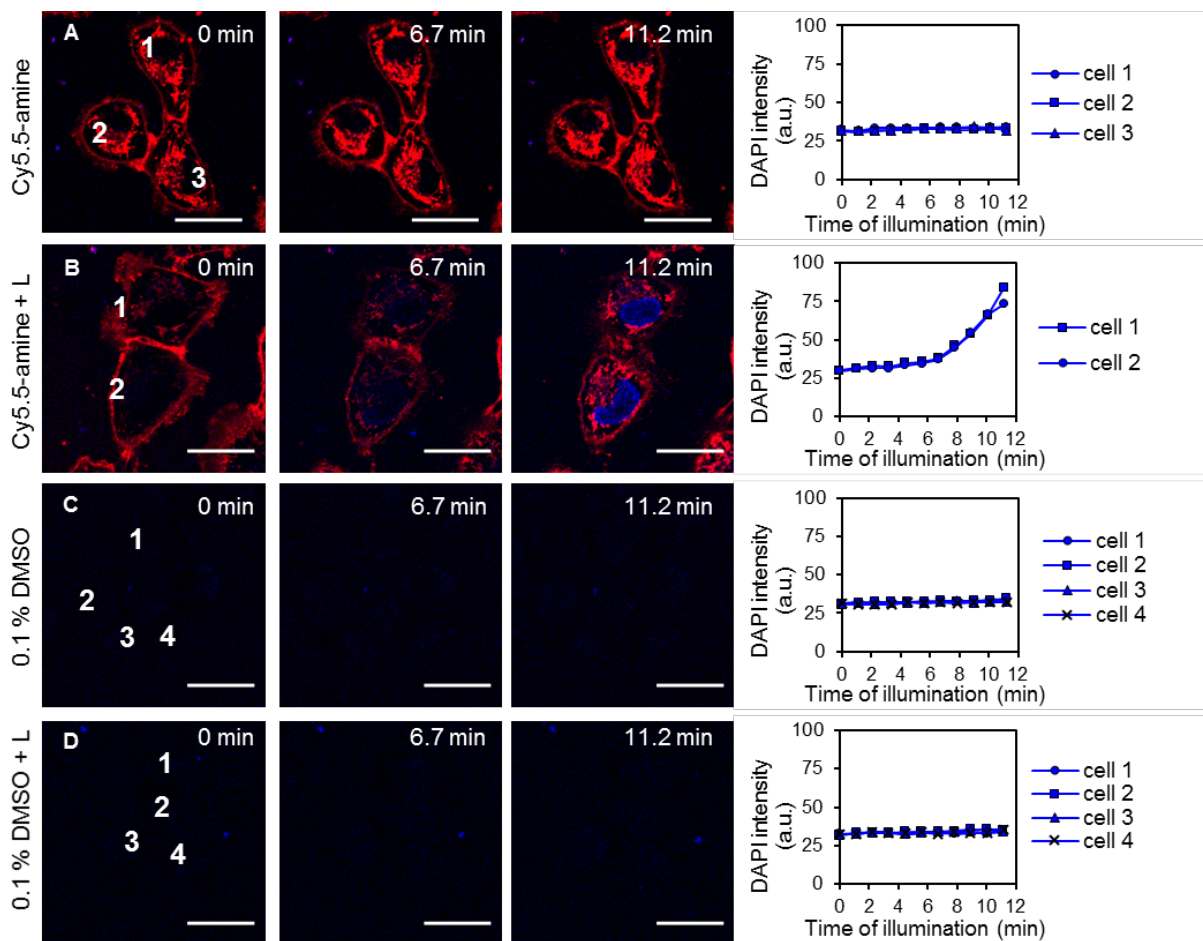


Figure S9. Cell membrane permeabilization by plasmon-activated MJH in A375 cells and direct imaging of Cy5.5-amine. The permeabilization of DAPI into the cells was recorded as a function of time (rightmost column). **A)** Cells in the presence of 2 μM Cy5.5-amine without laser irradiation. **B)** Cells in the presence of 2 μM Cy5.5-amine with 640 nm laser irradiation, 25% power (210 μW). **C)** Cells in the presence of 0.1% DMSO without laser irradiation. **D)** Cells in the presence of 0.1% DMSO with 640 nm laser irradiation. The irradiation times are shown in each image. For the activation of the MJH effect, the cells were irradiated at $\lambda_{\text{ex}} = 640$ nm, 25% power (210 μW). The pictures were recorded every 1 min. Cy5.5-amine can be observed in red bound to the plasma membrane, $\lambda_{\text{ex}} = 640$ nm, and $\lambda_{\text{em}} = 663\text{-}738$ nm. Loading concentration of DAPI: $C_{\text{loading}} = 1$ μM , $\lambda_{\text{ex}} = 405$ nm, and $\lambda_{\text{em}} = 425\text{-}475$ nm. The cyanines were added into the cell culture

and quickly imaged and treated, typically taking ~ 7 min from the time the cyanine was added to the time the light treatment started. Representative confocal images of each condition are shown.

All scale bars = 25 μm .

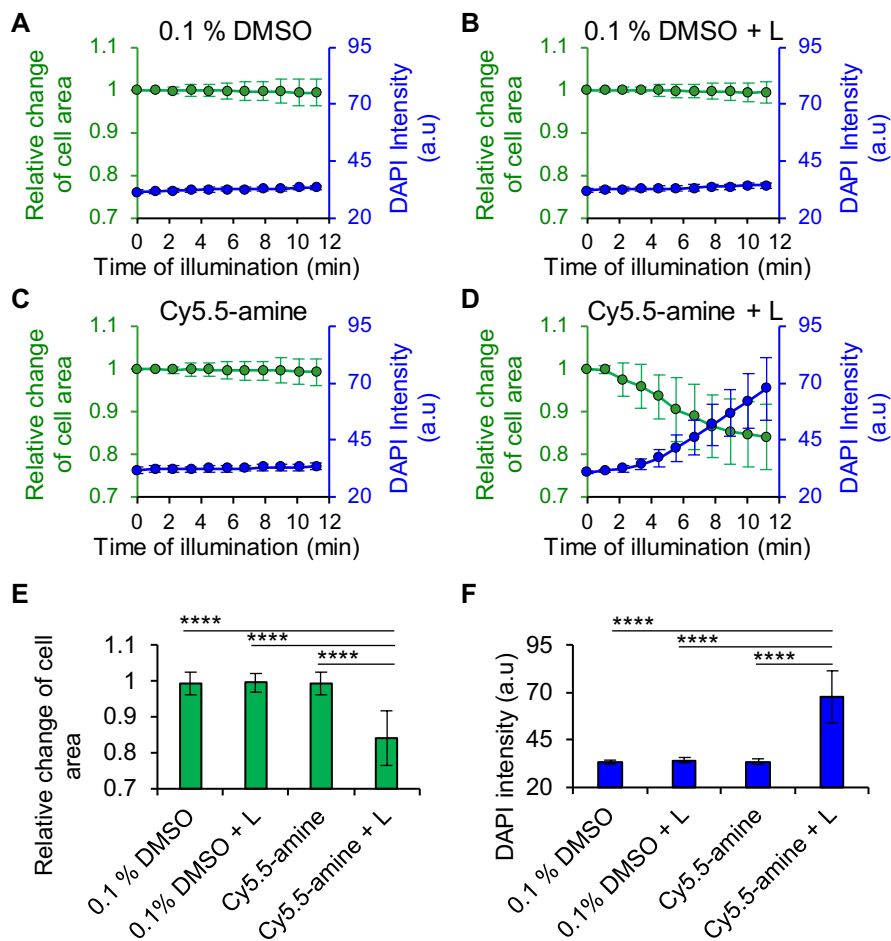


Figure S10. Cell membrane permeabilization by light-activated MJH in A375 cells. The permeabilization of DAPI into the cells and the size of the cells were recorded as a function of time. Four experiments were replicated, and 42 cells were analyzed for each experimental group. **A)** Cells in the presence of 0.1% DMSO control without laser irradiation. **B)** Cells in the presence of 0.1% DMSO with 640 nm laser irradiation. **C)** Cells in the presence of 2 μM Cy5.5-amine without laser irradiation. **D)** Cells in the presence of 2 μM Cy5.5-amine with 640 nm laser irradiation. For the activation of the MJH effect, the cells were irradiated at $\lambda_{\text{ex}} = 640$ nm, 25%

power (210 μW) in the confocal microscope. **E**) Relative change of the cell area at the end of the measurement (time = 11.2 min). The relative area of the cell was calculated by dividing the area at any time over its initial area at 0 min. **D**) Fluorescence intensity of DAPI at the end of the measurement (time = 11.2 min). In all panels, the data are presented as the mean \pm s.d. ($n = 42$). The P values were calculated by the two-tailed t-test: **** $P < 0.0001$. Statistical significance: $P < 0.05$.

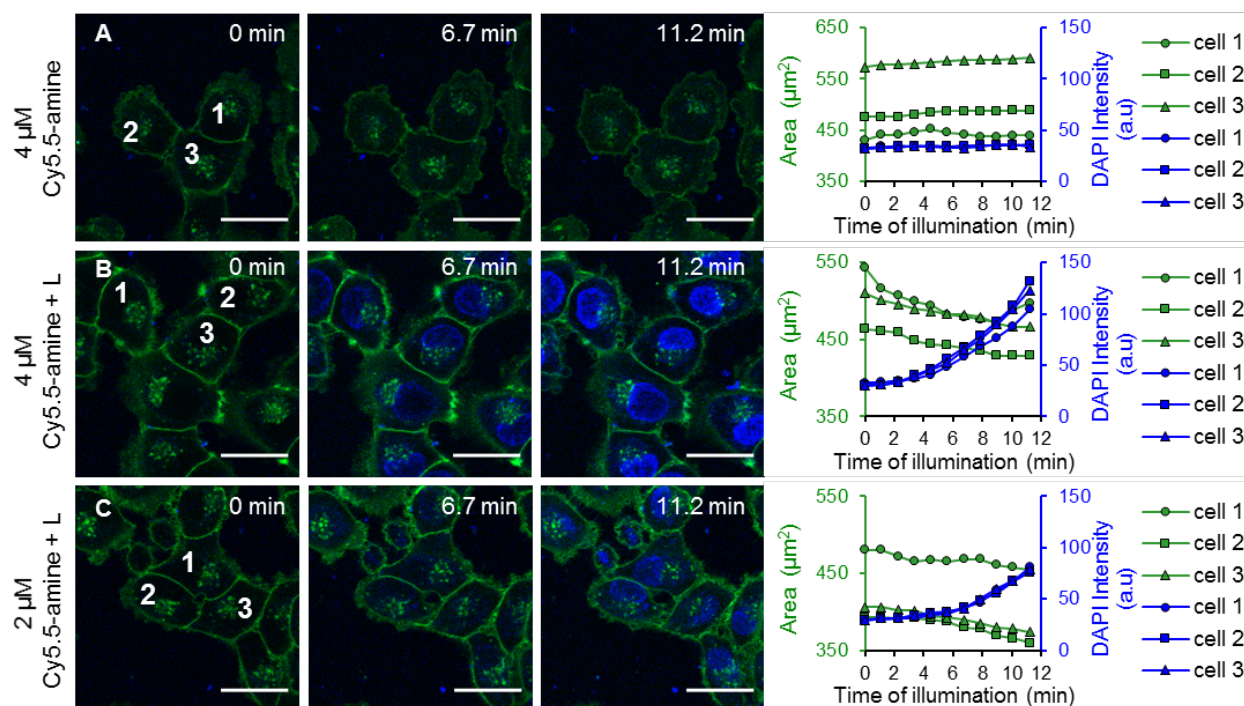


Figure S11. Cell membrane permeabilization by plasmon-activated MJH in A375 cells. The permeabilization of DAPI into the cells and the size of the cells were recorded as a function of time (rightmost column). **A**) Cells in the presence of 4 μM Cy5.5-amine without laser irradiation. **B**) Cells in the presence of 4 μM Cy5.5-amine with 640 nm laser irradiation. **C**) Cells in the presence of 2 μM Cy5.5-amine with 640 nm laser irradiation. The irradiation times are shown in each image. For the activation of the MJH effect, the cells were irradiated at $\lambda_{\text{ex}} = 640 \text{ nm}$, 25%

power (210 μW). The pictures were recorded every 1 min. CellMask Green is a cell membrane stain, $C_{\text{loading}} = 5 \mu\text{g mL}^{-1}$ for 30 min, $\lambda_{\text{ex}} = 488 \text{ nm}$, and $\lambda_{\text{em}} = 500\text{-}550 \text{ nm}$. Loading concentration of DAPI: $C_{\text{loading}} = 1 \mu\text{M}$, $\lambda_{\text{ex}} = 405 \text{ nm}$, and $\lambda_{\text{em}} = 425\text{-}475 \text{ nm}$. The cyanines were added into the cell culture and quickly imaged and treated, typically taking $\sim 7 \text{ min}$ from the time the cyanine was added to the time the light treatment started. Representative confocal images of each condition are shown. All scale bars = 25 μm .

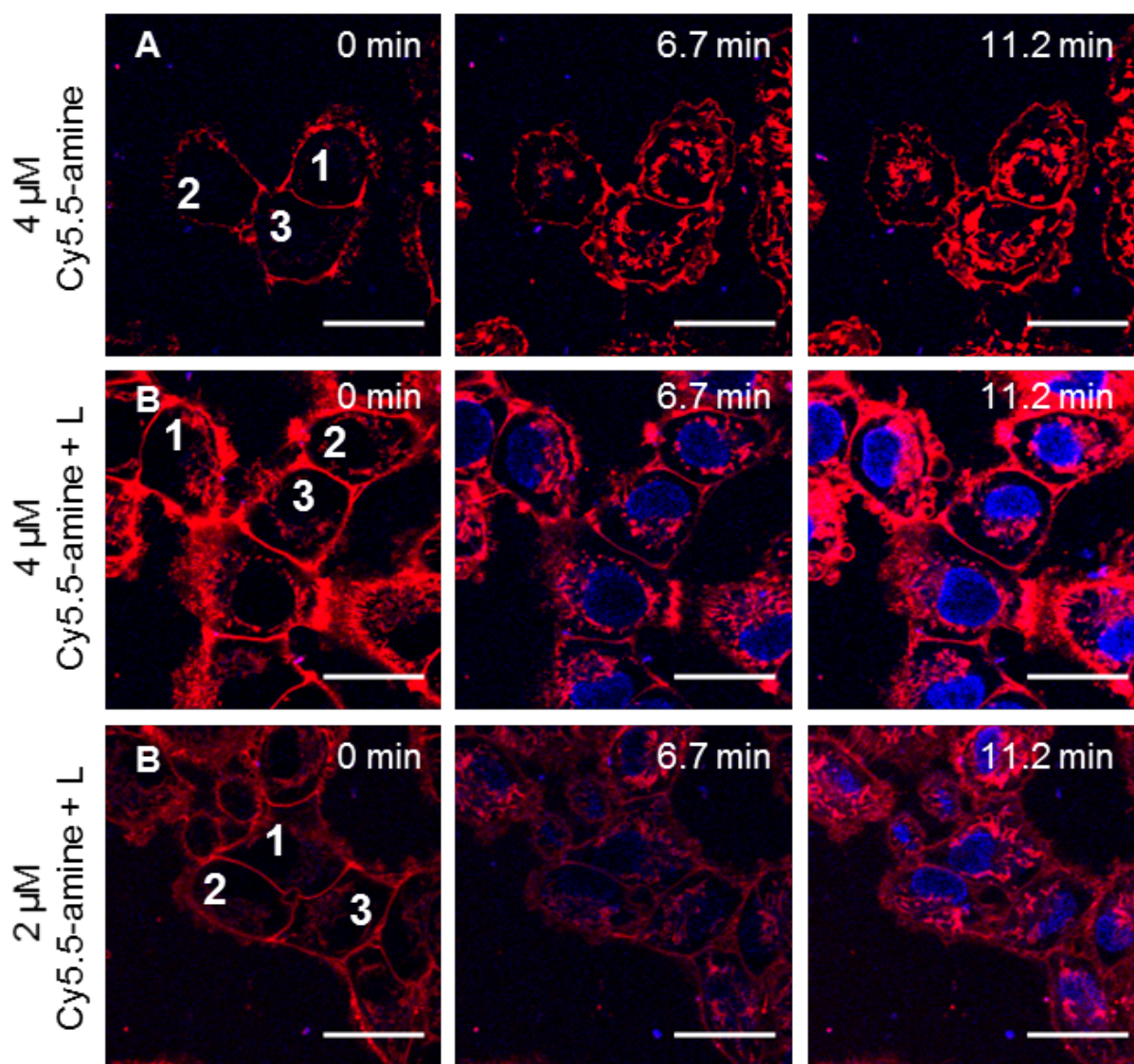


Figure S12. Cell membrane permeabilization by plasmon-activated MJH in A375 cells and direct imaging of Cy5.5-amine. The cells correspond to the same conditions and experiment in Figure S4, respectively. Here the Cy5.5-amine is visualized. **A)** Cells in the presence of 4 μM Cy5.5-amine without laser irradiation. **B)** Cells in the presence of 4 μM Cy5.5-amine with 640 nm laser irradiation. **C)** Cells in the presence of 2 μM Cy5.5-amine with 640 nm laser irradiation. The irradiation times are shown in each image. For the activation of the MJH effect, the cells were irradiated at $\lambda_{\text{ex}} = 640$ nm, 25% power (210 μW). The pictures were recorded every 1 min. Cy5.5-amine can be observed in red bound to the plasma membrane, $\lambda_{\text{ex}} = 640$ nm, and $\lambda_{\text{em}} = 663\text{-}738$ nm. Loading concentration of DAPI: $C_{\text{loading}} = 1$ μM , $\lambda_{\text{ex}} = 405$ nm, and $\lambda_{\text{em}} = 425\text{-}475$ nm. The cyanines were added into the cell culture and immediately imaged and treated, typically taking ~ 7 min from the time the cyanine was added to the time the light treatment started. Representative confocal images of each condition are shown. All scale bars = 25 μm .

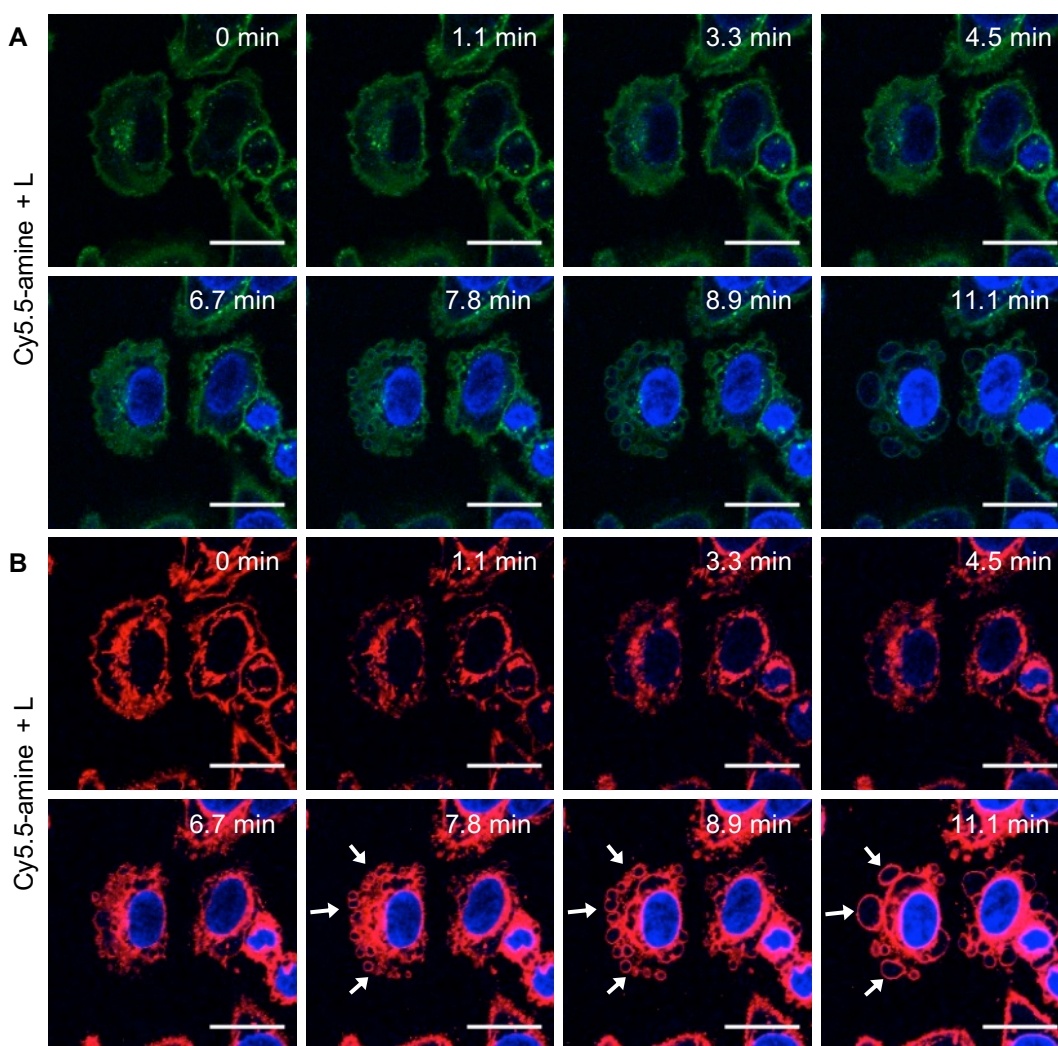


Figure S13. Cell membrane destruction by plasmon-driven MJH in A375 cells. The permeabilization of DAPI into the cells and membrane destruction were recorded over the time. **A)** Cells in the presence of 4 μM Cy5.5-amine with laser irradiation and imaging of CellMask in green channel. CellMask Green is a cell membrane stain, $C_{\text{loading}} = 5 \mu\text{g mL}^{-1}$ for 30 min, $\lambda_{\text{ex}} = 488 \text{ nm}$, and $\lambda_{\text{em}} = 500\text{-}550 \text{ nm}$. **B)** Cells in the presence of 4 μM Cy5.5-amine with 640 nm laser irradiation and imaging of Cy5.5-amine in red channel. Cy5.5-amine can be observed in red bound to the plasma membrane, $\lambda_{\text{ex}} = 640 \text{ nm}$, and $\lambda_{\text{em}} = 663\text{-}738 \text{ nm}$. The irradiation times are shown in each image. For the activation of the MJH effect, the cells were irradiated at $\lambda_{\text{ex}} = 640 \text{ nm}$, 25% power (210 μW). The pictures were recorded every 1 min. Loading concentration of DAPI: C_{loading}

= 1 μ M, λ_{ex} = 405 nm, and λ_{em} = 425-475 nm. The cyanines were added into the cell culture and immediately imaged and treated, typically taking \sim 7 min from the time the cyanine was added to the time the light treatment started. Representative confocal images of each condition are shown. All scale bars = 25 μ m.

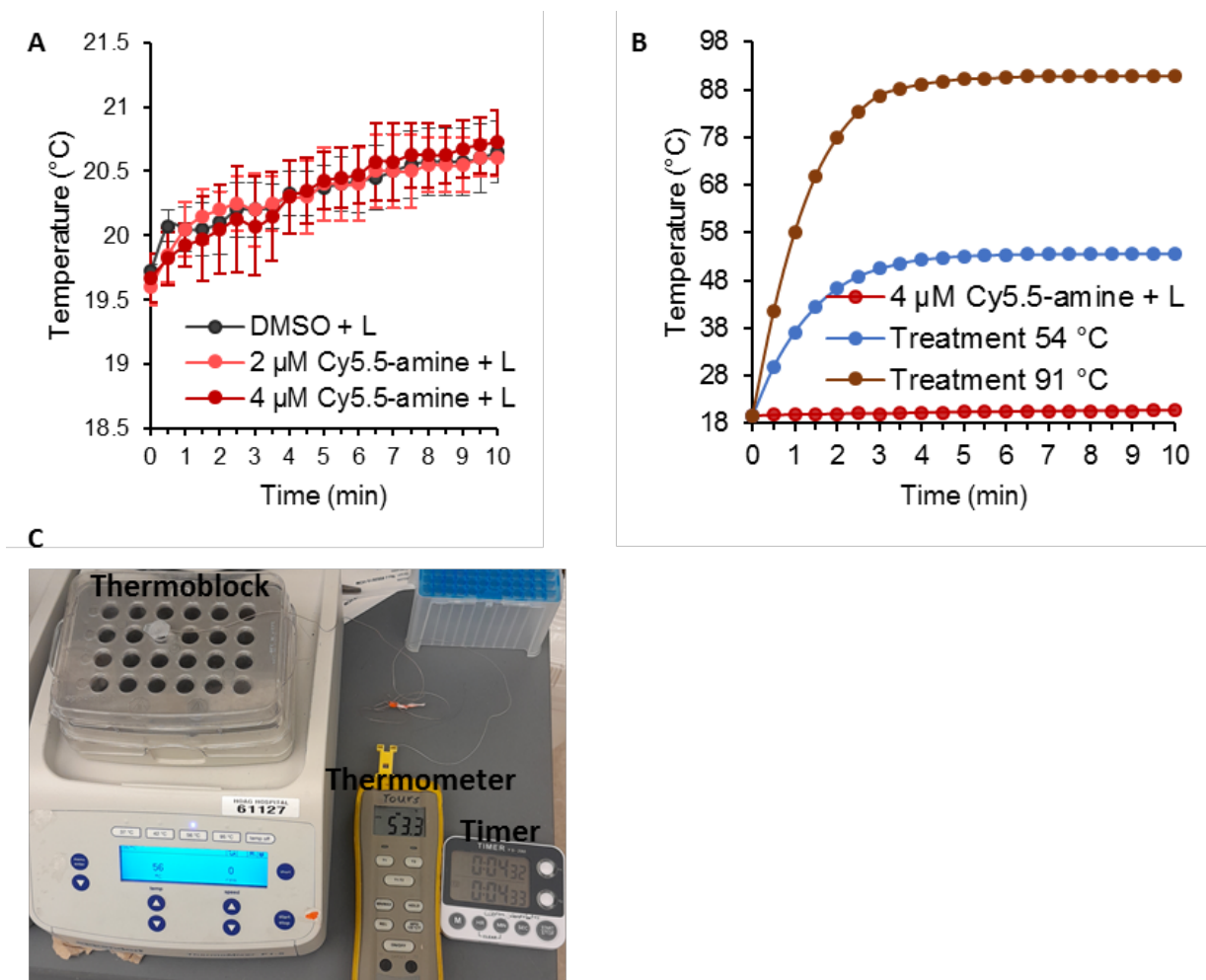


Figure S14. Temperature of the cell suspension under light treatment versus thermal treatments. **A)** The temperature curve of the A375 cells suspension under light activated Cy5.5-amine (n = 4 measurements on independent samples). **B)** Temperature curve of the cell suspension under thermal treatment and comparison with the light activated Cy5.5-amine treatment (n = 3 measurements on independent samples). **C)** Picture of the setup utilized for the thermal treatments.

The sample is contained in a 1.5 mL plastic tube and the thermometer probe is inserted into the solution. The exact temperature in the solution is recorded overtime.

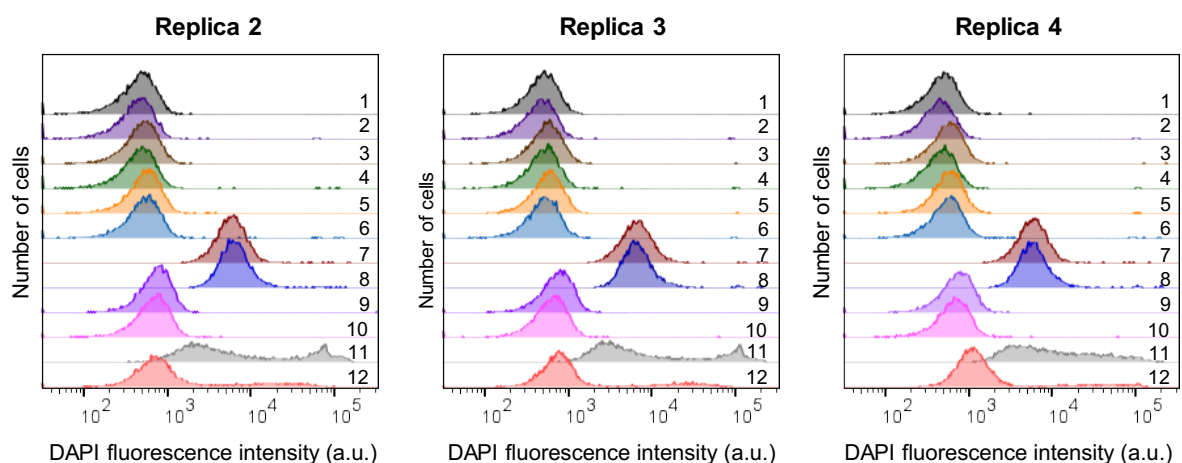


Figure S15. Flow cytometry analysis shows that ROS scavengers do not inhibit the permeabilization of cells by plasmon-driven MJH. Cells treated with 0.1% DMSO only (1), cells treated with 0.1% DMSO + 100 mM thiourea + 2.5 mM sodium azide (2), cells treated with 0.1% DMSO + light (3), cell treated with 0.1% DMSO + 100 mM thiourea + 2.5 mM sodium azide + light (4), cells treated with 4 μ M Cy5.5-amine (5), cells treated with 4 μ M Cy5.5-amine + 100 mM thiourea + 2.5 mM sodium azide (6), cells treated with 4 μ M Cy5.5-amine + light (7), cells treated with 4 μ M Cy5.5-amine + 100 mM thiourea + 2.5 mM sodium azide + light (8), cells treated with 50 mM H_2O_2 for 10 min (9), and cells treated with 100 mM thiourea + 2.5 mM sodium azide + 50 mM H_2O_2 for 10 min (10), cells treated with 50 mM H_2O_2 for 1 h (11), and cells treated with 100 mM thiourea + 2.5 mM sodium azide + 50 mM H_2O_2 for 1 h (12). Light treatments consisted of 630 nm LED at 80 mW cm^{-2} for 10 min. All the cell suspensions for this study contained 0.1% DMSO which is used to pre-solubilize the cyanine MJH in 4 mM stock solution.

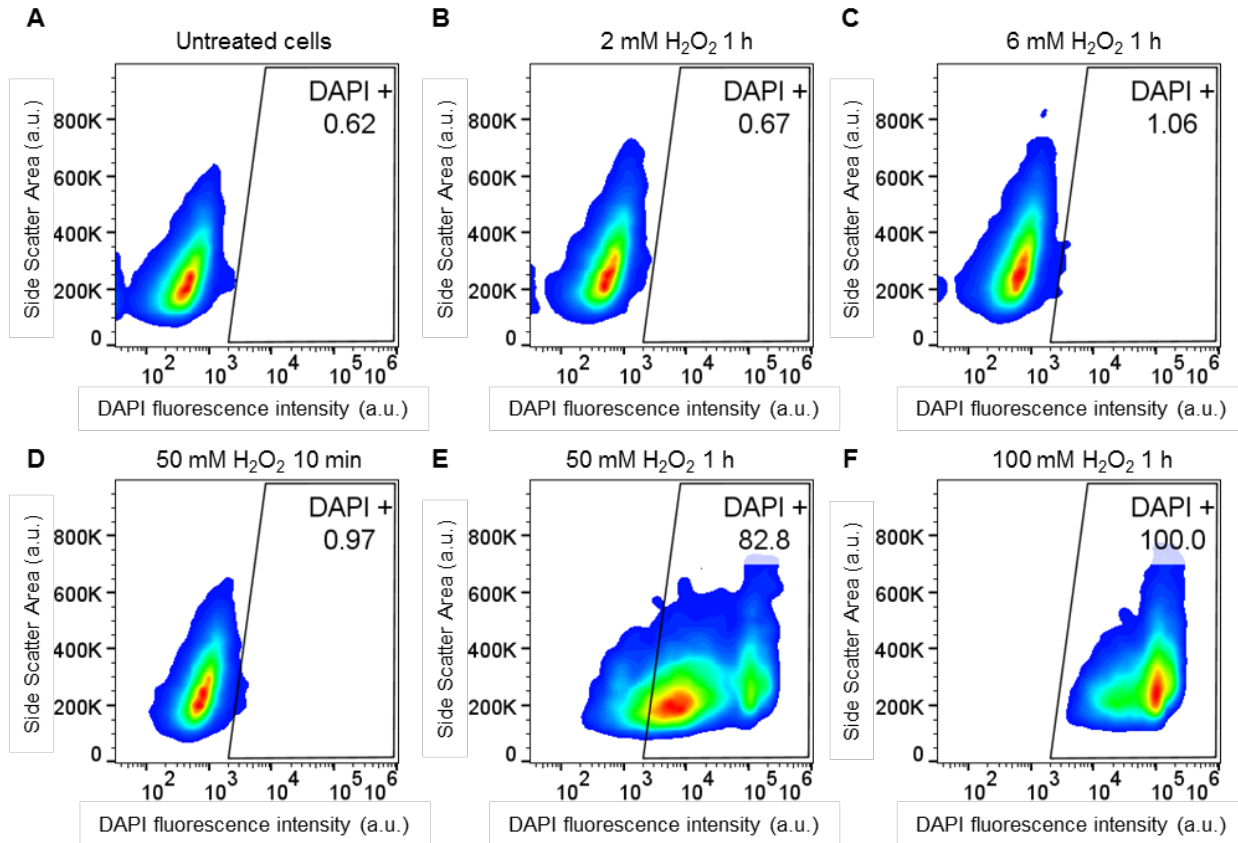


Figure S16. Relatively high concentrations of ROS and long times of exposure are needed for permeabilization of the cellular membranes. Flow cytometry analysis is utilized to measure the membrane permeability by DAPI staining in A375 cells. **A)** Untreated cells, **B)** 2 mM H₂O₂ was added and incubated for 1 h at 37 °C, **C)** 6 mM H₂O₂ was added and incubated for 1 h at 37 °C, **D)** 50 mM H₂O₂ was added and incubated for 10 min at 37 °C, **E)** 50 mM H₂O₂ was added and incubated for 1 h at 37 °C, **F)** 100 mM H₂O₂ was added and incubated for 1 h at 37 °C. Two independent experiments were replicated (n=2) and same results were obtained.

Molecular displacement in molecular jackhammers and implications in force calculation and membrane rupture.

Vibrational frequency from the harmonic model

In the harmonic approximation, a vibrating diatomic molecule is modeled as two masses connected by a spring with a force constant k . The vibrational frequency is given by:

$$\nu = \frac{1}{2\pi} \sqrt{\frac{k}{\mu}}$$

where:

k is the bond force constant (N/m),

μ is the reduced mass of the system, given by:

$$\mu = \frac{m_1 m_2}{m_1 + m_2}$$

where m_1 and m_2 are the atomic masses of the two atoms in the molecule.

Vibrational energy and displacement

The energy levels of a quantum harmonic oscillator are given by:

$$E_n = \left(n + \frac{1}{2}\right) h \nu$$

where h is Planck's constant (6.626×10^{-34} J·s), and n is the vibrational quantum number.

For the first vibrational state ($n = 1$), the energy is:

$$E_1 = \frac{3}{2} h \nu$$

The displacement x corresponding to this vibrational energy can be estimated from the zero-point amplitude, derived from the quantum mechanical harmonic oscillator:

$$x_1 = \sqrt{\frac{h}{4\pi^2\mu\nu}}$$

Maximum outward force

The restoring force in a harmonic oscillator follows Hooke's Law:

$$F = -kx$$

The maximum outward force is when the displacement reaches its maximum at x_1 , so:

$$F_{max} = kx_1 = k \sqrt{\frac{h}{4\pi^2\mu\nu}}$$

Normal modes (large molecules) vs. Local modes (diatomic)

In diatomic molecules, vibrations can be treated as simple harmonic motion involving just one bond. In larger molecules, vibrations occur as normal modes, where multiple atoms move collectively in a correlated way. Each normal mode still behaves approximately as a harmonic oscillator, meaning the equations can be applied, but the effective force constant k_{eff} and the effective reduced mass μ_{eff} for that mode is needed.

Effective force constant k_{eff}

For complex molecules, the force constant is not just a single bond strength but depends on the molecular structure. Computational methods (DFT, normal mode analysis) or experimental IR/Raman spectra can provide approximate values.

Effective reduced mass μ_{eff}

For a normal mode involving multiple atoms, the reduced mass is:

$$\mu_{\text{eff}} = \sum_i m_i \left(\frac{\Delta x_i}{\Delta X} \right)^2$$

where:

m_i is the atomic mass of the i th atom,

Δx_i is the displacement of the i th atom in the normal mode,

ΔX is the total displacement amplitude of the mode.

Applying the harmonic model in molecules

Once k_{eff} and μ_{eff} are determined, can be used:

$$\nu = \frac{1}{2\pi} \sqrt{\frac{k_{\text{eff}}}{\mu_{\text{eff}}}}$$

to get the vibrational frequency.

Similarly, the displacement for a quantum state ($n = 1$) is:

$$x_1 = \sqrt{\frac{h}{4\pi^2 \mu_{\text{eff}} \nu}}$$

and the maximum force is:

$$F_{\text{max}} = k_{\text{eff}} \cdot x_1$$

Important considerations on the problem of calculating displacements with the harmonic model in molecules.

It is important to clarify that these equations for the harmonic model are expected to be inaccurate for calculations in molecules since the reduced mass of the molecule is treated in the calculations as if this mass is concentrated on two single points of the harmonic oscillator model. The equations for the harmonic model are valid for diatomic molecules, or two atoms connected through a single bond. Here, we are only doing these approximations to extract some values

regarding the force exerted by the vibrational frequency obtained from the Raman spectrum. Indeed, the displacements will be even smaller in the molecules than in diatomic pairs since the displacements are inversely proportional to the effective reduced mass. In molecules, due to their larger size, the reduced mass will be larger than in diatomic pairs. Therefore, the displacements estimated by this model are not accurate for the large amplitude global vibration in molecules. Overall, the harmonic oscillator approximation underestimates the molecular displacement, especially in excited-state dynamics where electron-phonon coupling plays a significant role.

The harmonic model predicts a strong outward force enough to rupture the membranes even when the displacements are very small.

Even though the harmonic model inaccurately predicts very small displacements for molecules, the calculated maximum outward force in Cy5.5 is ~1700 times higher than the force previously calculated, as will be shown below.

A normal mode with 1330 cm^{-1} Raman shift is measured experimentally. Here, we apply the equations of the harmonic model to calculate the force constant for the normal mode, the displacement, and the maximum outward force. We do this in two scenarios for comparison: 1) approximating the normal mode as C-C stretching mode to calculate the exact reduced mass of the C-C pair and 2) calculating the approximate effective reduced mass of the whole Cy5.5 molecule.

Convert the Raman shift to frequency.

The Raman spectrum gives the vibrational frequency in wavenumbers ($\tilde{\nu}$) with units of cm^{-1} :

$$\tilde{\nu} = 1330\text{ cm}^{-1}$$

Convert this to frequency in Hz using:

$$\nu = \tilde{\nu} \times c$$

where:

$$c = 2.998 \times 10^{10} \text{ cm/s (speed of light).}$$

$$\nu = (1330 \text{ cm}^{-1}) \times (2.998 \times 10^{10} \text{ cm/s})$$

$$\nu = 3.99 \times 10^{13} \text{ Hz}$$

Calculate the reduced mass for the C-C mode.

The reduced mass μ is:

$$\mu = \frac{m_1 m_2}{m_1 + m_2}$$

where m_1 and m_2 are the atomic masses. Suppose the vibration corresponds to a C-C stretch, then:

$$\text{Carbon atomic mass: } m_C = 12.01 \text{ amu}$$

$$\text{Convert to kg: } 1 \text{ amu} = 1.6605 \times 10^{-27} \text{ kg}$$

$$\mu = \frac{(12.01)(12.01)}{12.01 + 12.01} \times (1.6605 \times 10^{-27} \text{ kg})$$

$$\mu = 9.97 \times 10^{-27} \text{ kg}$$

Calculate the effective force constant for the C-C mode.

The vibrational frequency is related to the force constant by:

$$\nu = \frac{1}{2\pi} \sqrt{\frac{k_{\text{eff}}}{\mu}}$$

Rearrange to solve for k_{eff} :

$$k_{\text{eff}} = (2\pi\nu)^2 \mu$$

Substituting values:

$$k_{\text{eff}} = (2\pi \times 3.99 \times 10^{13})^2 \times (9.97 \times 10^{-27})$$

$$k_{\text{eff}} = 627.5 \text{ N/m}$$

Calculate the displacement for the C-C mode.

The zero-point amplitude (displacement for $n = 1$) in a quantum harmonic oscillator is given by:

$$x_1 = \sqrt{\frac{h}{4\pi^2 \mu \nu}}$$

where:

$$h = 6.626 \times 10^{-34} \text{ J}\cdot\text{s (Planck's constant),}$$

μ is the reduced mass (from the previous step, $9.97 \times 10^{-27} \text{ kg}$),

$$\nu = 3.99 \times 10^{13} \text{ Hz.}$$

Substituting Values:

$$x_1 = \sqrt{\frac{6.626 \times 10^{-34}}{4\pi^2(9.97 \times 10^{-27})(3.99 \times 10^{13})}}$$
$$x_1 = 6.5 \times 10^{-12} \text{ m} = 6.5 \text{ pm}$$

Calculate the effective reduced mass for the whole molecule.

For a collective breathing mode involving the entire Cy5.5 molecule:

The molecular weight of Cy5.5 is 483 g/mol.

Convert this to kg per molecule:

$$m_{\text{molecule}} = \frac{483}{6.022 \times 10^{23}} \text{ g}$$
$$m_{\text{molecule}} = 8.02 \times 10^{-25} \text{ kg}$$

Since normal modes involve multiple atoms vibrating together, the effective reduced mass is typically 5–15% of the total mass in large organic molecules.

Using an estimated 10% of the molecular mass:

$$\mu_{\text{eff}} \approx 0.1 \times 8.02 \times 10^{-25}$$

$$\mu_{\text{eff}} \approx 8.02 \times 10^{-26} \text{ kg}$$

Comparison:

- C–C bond reduced mass: $9.97 \times 10^{-27} \text{ kg}$
- Cy5.5 breathing mode: $8.02 \times 10^{-26} \text{ kg}$
- Ratio: 8× larger than a single C–C bond mode.

The effective mass of the molecule is much larger than the diatomic case.

Calculate the effective displacement for the whole molecule.

Substituting values:

$$x_1 = \sqrt{\frac{6.626 \times 10^{-34}}{4\pi^2(8.02 \times 10^{-26})(3.99 \times 10^{13})}}$$
$$x_1 = 2.29 \times 10^{-12} \text{ m} = 2.29 \text{ pm}$$

Comparison:

- C–C bond vibration: 6.5 pm
- Cy5.5 breathing mode: 2.29 pm
- Ratio: Cy5.5 displacement is $\sim 3\times$ smaller than C–C vibration

The harmonic model is for diatomic molecules. It could be accurate for the C-C bond vibration. However, this model is not accurate for the global displacement of the molecule for the reasons mentioned before.

Calculate the force constant for the whole molecule.

The force constant is related to the vibrational frequency by:

$$k_{\text{eff}} = (2\pi\nu)^2 \mu_{\text{eff}}$$

Substituting values:

$$k_{\text{eff}} = (2\pi \times 3.99 \times 10^{13})^2 \times (8.02 \times 10^{-26})$$
$$k_{\text{eff}} = 504.5 \text{ N/m}$$

Comparison:

- C–C bond force constant: 627.5 N/m
- Cy5.5 breathing mode: 504.5 N/m
- Ratio: Cy5.5 force constant is $\sim 20\%$ smaller than a single C–C bond.

Calculate the maximum force for the whole Cy5.5 molecule.

The maximum force exerted is:

$$F_{max} = k_{eff} \cdot x_1$$

Substituting values:

$$F_{max} = (504.5) \times (2.29 \times 10^{-12})$$
$$F_{max} = 1.15 \times 10^{-9} \text{ N}$$

Comparison:

- C–C bond vibration: $4.1 \times 10^{-9} \text{ N} = 4.1 \text{ nN}$
- Cy5.5 breathing mode: $1.15 \times 10^{-9} \text{ N} = 1.15 \text{ nN}$
- Ratio: The maximum force is $\sim 3.5\times$ smaller than for the C–C vibration.

Discussion of the results and implications.

The harmonic model is valid for diatomic molecules but not for large molecules. However, for this discussion, let us assume the harmonic model calculations are correct for molecules. The calculated force (1.15 nN) would be enough to rupture the membrane. In the main text, we discussed that the mechanical stress required to rupture most membranes is 1-30 mNm⁻¹. If we take the calculated force of 1.15 nN and apply it to the 2.29 pm displacement, then we obtain a mechanical stress of 504.5 Nm⁻¹, which is ~ 17000 -fold larger than the mechanical stress required to rupture most membranes. This displacement of 2.29 pm, calculated from the harmonic model is not accurate. We are only showing this analysis to indicate the inconsistencies with the harmonic model for molecules. This underestimated displacement does not represent the amplitude of the whole molecule vibration in molecular jackhammers. The harmonic oscillator approximation underestimates the molecular displacement, especially in excited-state dynamics where electron-phonon coupling plays a significant role. Most likely, the correct way to interpret this is that the force is not localized to the atomic displacement, but rather the force is exerted radially at a certain distance beyond the physical displacement of the atoms. In general, the atoms never touch each

other physically to experience the intermolecular forces (e.g., van der Waals forces). This type of force can be described with a Lennard-Jones potential, a type of force field that describes the intermolecular forces, which contains a long-range interaction term that decays with the distance. In the same way, the mechanical force exerted by the molecular jackhammer could be experienced by the surrounding molecules at a distance, and decays radially as the distance increases. The same is valid for the macroscopic analogy of the jackhammer in construction. The mechanical force is not confined exclusively to the tip of a real-world jackhammer, but rather the force radiates at a distance and can break the concrete beyond the physical point of contact of the jackhammer. Therefore, rather than confining the calculation to a specific distance, we should ask the question: What force would be exerted at different distances?

In the main text of the manuscript, for the 1330 cm^{-1} Raman shift from the Cy5.5 spectrum, a force of 0.026 nN is estimated at 1 nm , and this generates a mechanical stress of 26 mNm^{-1} at 1 nm , which is enough to rupture the membrane. The distance of 1 nm is a reasonable starting point for the calculation since the dimension of Cy5.5 molecule is $\sim 1\text{ nm}$. Upon excitation of the vibronic mode, the molecule expands and contracts as if the molecule is breathing. Then, the force generated is distributed side to side along the $\sim 1\text{ nm}$ molecule since the molecule is expanding and contracting, and the force can be exerted radially to the surroundings due to the vibrational displacement and to the short-range repulsive forces and long-range attractive forces. If the distance is smaller than 1 nm , then the mechanical stress (force over the distance) becomes larger. Then, in all scenarios for distances $\sim 1\text{ nm}$ or shorter, the exerted force is estimated to be enough to rupture the membrane. For context, the intermolecular distance between phospholipid molecules in a membrane is $\sim 0.25\text{-}0.3\text{ nm}$. Then, the force at 1 nm from the molecular jackhammer can be exerted on the adjacent molecule. Let us suppose the distance is 0.1 nm , then the mechanical stress

will be 10-fold higher than at 1 nm; 0.01 nm (10 pm) will result in 100-fold higher mechanical stress. The shorter the distance, the higher the mechanical stress. At longer distances, the mechanical stress will be weaker. This means that the force and mechanical stress will be stronger at shorter distances from the molecule and weaker at longer distances. This makes sense, given the macroscopic analogy of the jackhammer in construction. The force and mechanical stress will be higher closer to the tip of the jackhammer. It is not a large amplitude that breaks the concrete but rather a fast, short amplitude vibration.

An estimate of the maximum molecular displacement of the whole molecule vibration.

This so-called whole molecule vibration in molecular jackhammers is also known as the breathing mode in carbon nanotubes. This is well-studied in carbon nanotubes. The breathing mode (radial breathing mode) of an excited carbon nanotube (CNT) refers to the vibrational mode where the entire tube expands and contracts radially. The molecular displacement of this mode depends on the tube's diameter, excitation energy, and the strength of the electron-phonon coupling. Here, will be shown a clear example of how the harmonic oscillator model significantly underestimates the molecular displacement by a factor of ~20-100-fold smaller in carbon nanotubes. Applying the harmonic oscillator model for a 1 nm CNT, rough estimates give molecular displacements of ~1-10 pm, like the molecular displacement estimated for the Cy5.5 (2.3-6.5 pm).

Studies on CNTs and π -conjugated systems like fullerenes and graphene nanoribbons suggest that the molecular displacement of the radial breathing mode in the excited state is significantly larger than ground-state vibrational estimates. Experimental and theoretical studies indicate that the excited-state displacement for the radial breathing mode in CNTs is typically in the range of 50-500 pm (0.05–0.5 Å), depending on the CNT diameter and excitation energy.⁵ For

small-diameter CNTs (~1 nm), calculations have shown radial breathing mode displacements of ~100-200 pm in the excited state, significantly larger than the ~1-10 pm estimate from a simple harmonic model.

For a ~1 nm molecular jackhammer, a breathing mode displacement of ~100 pm (0.1 nm) is feasible. This value is at the lower bound range for π -conjugated carbon systems of similar size to be conservative in our estimations. Then, for the 1330 cm^{-1} Raman shift from the Cy5.5 spectrum, this is the breathing mode; a force of 0.26 nN is estimated at a displacement of 0.1 nm. Applying this force over 1 nm, we estimate a mechanical stress of 260 mNm^{-1} , which is ~10 times higher than the mechanical stress required to rupture most membranes. In principle, this is possible through force field interactions, the long-range intermolecular interactions. As mentioned before, the distance between phospholipid molecules in membranes is ~0.25-0.3 nm. The distance between molecular jackhammers and phospholipid alkyl chains can be in that range. The long-range intermolecular interactions operate at these distances, so mechanical forces can be exerted on the adjacent molecule. This is another way to calculate the force exerted by the molecular jackhammer and confirms that the molecular jackhammer should be sufficient to rupture the membrane, here by a factor of ~10 times higher than we estimated in the main manuscript. Both estimations can be considered valid after thoroughly discussing the context and implications of both. The important point is that in both scenarios, the mechanical stress is sufficient to rupture the membrane.

References

- 1 H. Mustroph and A. Towns, *ChemPhysChem*, 2018, **19**, 1016–1023.
- 2 C. Ayala-Orozco, D. Galvez-Aranda, A. Corona, J. M. Seminario, R. Rangel, J. N. Myers and J. M. Tour, *Nat. Chem.*, 2024, **16**, 456–465.

- 3 C. Ayala-Orozco, G. Li, B. Li, V. Vardanyan, A. B. Kolomeisky and J. M. Tour, *Adv. Mater.*, 2024, **36**, 2309910.
- 4 F. Schneider, D. Ruhlandt, I. Gregor, J. Enderlein and A. I. Chizhik, *J. Phys. Chem. Lett.*, 2017, **8**, 1472–1475.
- 5 M. Machón, S. Reich and C. Thomsen, *Phys. Status Solidi (B)*, 2006, **243**, 3166–3170.